

Cite this: Phys. Chem. Chem. Phys., 2011, **13**, 5687–5695

PAPER www.rsc.org/pccp

Interlayer interaction and relative vibrations of bilayer graphene

Irina V. Lebedeva,* abc Andrey A. Knizhnik, bc Andrey M. Popov, d Yurii E. Lozovik da and Boris V. Potapkin bc

Received 21st November 2010, Accepted 17th January 2011

DOI: 10.1039/c0cp02614j

The van der Waals corrected first-principles approach (DFT-D) is for the first time applied for investigation of interlayer interaction and relative motion of graphene layers. A methodological study of the influence of parameters of calculations with the dispersion corrected and original PBE functionals on characteristics of the potential relief of the interlayer interaction energy is performed. Based on the DFT-D calculations, a new classical potential for interaction between graphene layers is developed. Molecular dynamics simulations of relative translational vibrations of graphene layers demonstrate that the choice of the classical potential considerably affects dynamic characteristics of graphene-based systems. The calculated low values of the Q-factor for these vibrations $Q \approx 10-100$ show that graphene should be perfect for the use in fast-responding nanorelays and nanoelectromechanical memory cells.

Introduction

In addition to zero-dimensional and one-dimensional carbon nanostructures, fullerenes and carbon nanotubes, a novel two-dimensional carbon nanostructure, graphene, discovered recently. The experimental data suggest that few-layer graphene possesses a number of remarkable properties, which open the way for a variety of applications. Outstanding electrical, mechanical and chemical properties of graphene have been utilized in flexible transparent electrodes used recently in a fully functional touch-screen panel device. Stiff and flexible graphene oxide paper³ holds great promise for the use in fuel cell and structural composite applications.

A wide set of properties and applications of graphene is related to interaction between graphene layers. Thermal conductivity of graphene improves drastically with decreasing the number of layers.4 The structure of bilayer graphene membranes exhibits out-of-plane fluctuations (ripples).⁵ The possibility for graphene layers to form incommensurate configurations upon their relative rotation is responsible for such phenomena as superlubricity⁶⁻⁹ and fast diffusion¹⁰ of a graphene flake on a graphene layer. Experimentally observed self-retracting motion of graphite, i.e. retraction of graphite flakes back into the graphite stacks on their extension arising

For adequate consideration of the phenomena and nanoelectromechanical systems listed above and realistic simulation of graphene-based systems, exhaustive information on the interaction between graphene layers is necessary. In particular, accurate values of the interlayer binding energy, interlayer spacing, c-axis compressibility, magnitude of corrugation of the potential relief of the interlayer interaction energy, barrier to relative motion of graphene layers and frequencies of relative vibrations of graphene layers are required. Graphene layers consisting of covalently bound carbon atoms interact with each other by relatively weak dispersion forces. The weakness of these dispersion forces leads to experimental difficulties when measuring the mentioned physical quantities characterizing the interaction between graphene layers. The equilibrium interlayer distance, 16,17 c-axis compressibility 18 and phonon spectrum¹⁹ were experimentally measured for graphite with good accuracy. However, the data on the interlayer binding energy show significant scatter depending on the experimental approach.²⁰⁻²² No experimental data on the corrugation of the potential relief of the interlayer interaction energy are available. The value of the critical shear strength for graphite measured in the only known experiment²³ is related to macroscopic structural defects of the graphite sample. In the experiments with a graphene flake

from the van der Waals interaction, led to the idea of a gigahertz oscillator based on the telescopic oscillation of graphene layers. 11 A nanorelay based on the telescopic motion of nanotube walls 12,13 and a mass nanosensor based on the small translational vibrations of nanotube walls have been considered. 14,15 By analogy with these devices, a nanorelay based on the telescopic motion of graphene layers and a mass nanosensor based on the small translational vibrations of graphene layers can be proposed.

^a Moscow Institute of Physics and Technology, Institutskii pereulok 9, Dolgoprudny, Moscow Region 141701, Russia

^b RRC "Kurchatov Institute", Kurchatov Sq. 1, Moscow 123182, Russia

^c Kintech Lab Ltd, Kurchatov Sq. 1, Moscow 123182, Russia. E-mail: lebedeva@kintechlab.com, knizhnik@kintechlab.com; Fax: +7 499 1969992; Tel: +7 499 1969992

^d Institute of Spectroscopy, Fizicheskaya Str. 5, Troitsk, Moscow Region 142190, Russia. E-mail: am-popov@isan.troitsk.ru, lozovik@isan.troitsk.ru

moved by the tip of the friction force microscope, ⁶ only a small region of the potential relief of the interlayer interaction energy can be investigated. Therefore, *ab initio* calculations are particularly valuable for understanding the phenomena observed in graphene-based systems and providing the reference data for large-scale simulation techniques.

In the present paper, we for the first time use the van der Waals corrected first-principles approach for calculation of the interlayer interaction and relative motion of graphene layers. Based on this study, a new classical potential for interaction between graphene layers is developed. The potential is applied for molecular dynamics (MD) simulations of a nanoresonator based on the small relative translational vibrations of graphene layers.

The interaction of graphene layers at a distance of 3.4 Å has been difficult for theoretical description. The density functional theory (DFT) techniques based on the local density approximation (LDA) and generalized gradient density approximation (GGA) are unable to describe non-local dispersive interactions and, consequently, the cohesion of graphene layers.^{24–26} Therefore, it was proposed to supplement the LDA and GGA DFT calculations with an empirical long-range interaction term.^{24–27} Such a DFT-D approach made it possible to reproduce cohesive properties of graphite^{25,26,28-30} and interaction in systems of polycyclic aromatic molecules in different relative orientations. 29,31,32 Recently, a more rigorous approach was proposed by Dion et al.. 33 the van der Waals density functional (vdW-DF), which includes long-range dispersion using polarization properties of the almost uniform electron gas. However, as we show below (see Sec. 2), this less empirical correction gives results similar to the DFT-D approach.

We apply the recent DFT-D technique^{31,34} taking into account van der Waals interactions to investigate the potential relief of the interlayer interaction energy of bilayer graphene with high accuracy. The PBE-D functional,³⁰ which was shown to provide the values of the equilibrium interlayer distance, interlayer binding energy and *c*-axis compressibility of graphite closer to the experimental data^{16–18,22} than other DFT-D functionals,^{24,25,27,28} is used. We perform a methodological study of the influence of the parameters of calculations with the dispersion corrected and original functionals on the characteristics of the potential relief. This allows us to revise the results of the previous DFT calculations without the dispersion correction.^{35,36}

For simulation of graphene-based systems consisting of hundreds-thousands of atoms by the MD or the Monte Carlo method, an appropriate interatomic potential is required. The potential able to provide the sufficient overall cohesion of graphene layers and magnitude of corrugation fitted to the previous DFT calculations without the dispersion correction was suggested.^{35,36} We propose here a new potential for interlayer interaction of graphene layers and fit this potential to the results of our DFT-D calculations. The potential accurately reproduces both the experimental data on the interlayer binding energy, interlayer spacing, *c*-axis compressibility of graphite and the data obtained from the DFT-D calculations on the magnitude of corrugation of the interlayer interaction energy, barrier to relative motion of graphene

layers and frequency of the relative translational vibrations of graphene layers. Furthermore, we study the influence of the choice of the classical potential on dynamic behavior of graphene-based systems by the example of the nanoresonator based on small relative translational vibrations of graphene layers. Our molecular dynamics simulations demonstrate that dynamic characteristics of the nanoresonator described using the developed potential are strongly different from the characteristics of the systems described using the previously known potentials.

The paper is organized in the following way. The results of the DFT-D calculations of the potential relief of the interlayer interaction energy in bilayer graphene are presented in Sec. 2. In Sec. 3, we describe development of the new classical potential. The results of the MD simulations of the nanoresonator based on the small relative translational vibrations of graphene layers for different classical potentials are given in Sec. 4. Our conclusions are summarized in Sec. 5.

2. Potential relief of interaction energy of graphene layers

The recently developed DFT-D method^{31,34} taking into account van der Waals interactions was used to obtain the potential relief of the interlayer interaction energy of bilayer graphene with high accuracy. The periodic boundary conditions were applied to a 4.271 Å \times 2.466 Å \times 20 Å model cell. The VASP code³⁷ with the generalized gradient approximation (GGA) density functional of Perdew, Burke, and Ernzerhof, 38 in its original form (PBE) and corrected with the dispersion term (PBE-D),30 was used. The basis set consisted of plane waves with a maximum kinetic energy of 300-800 eV. The interaction of valence electrons with atomic cores was described using the projector augmented-wave method (PAW).39 The cutoff distance for van der Waals interactions was 200 Å. Integration over the Brillouin zone was performed using the Monkhorst-Pack method⁴⁰ with k-point grids from $12 \times 18 \times 1$ to $36 \times 54 \times 1$. The block Davidson scheme⁴¹ was used for iterative matrix diagonalization. The precision of convergence of the self-consistent field was 10⁻⁵ eV. A second-order Methfessel–Paxton smearing⁴² with a width of 0.1 eV was applied. In the calculations of the potential energy reliefs, one of the graphene layers was rigidly shifted parallel to the other. Account of structure deformation induced by the interlayer interaction was shown to be inessential for the shape of the potential relief for the interaction between graphene-like layers, such as the interwall interaction of carbon nanotubes⁴³ and the intershell interaction of carbon nanoparticles. 44,45

The calculated interlayer interaction energy of bilayer graphene as a function of the relative displacement of the graphene layers along the armchair direction at the equilibrium interlayer spacing is shown in Fig. 1 (see Fig. 2 of ref. 10 for the qualitative map of the potential relief of the interlayer interaction energy as a function of the relative displacement of the graphene layers in both in-plane directions). We found that minima $E_{\rm AB}$ of the interlayer interaction energy correspond to the AB-stacking of the layers, while maxima $E_{\rm AA}$ of the interlayer interaction energy correspond to the AA-stacking,

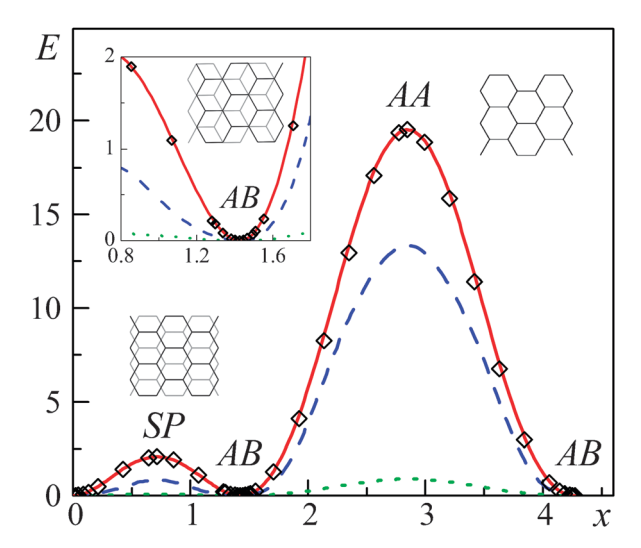


Fig. 1 Calculated interlayer interaction energy E (in meV per atom) of bilayer graphene at the equilibrium interlayer spacing as a function of the relative displacement x (in \mathring{A}) of the layers along the armchair direction for different potentials: Lennard-Jones potential (dotted line), Kolmogorov-Crespi potential (dashed line) and potential developed in the present work (solid line). The data obtained from the DFT-D calculations are shown with rhombs. The energy is given relative to the global energy minimum.

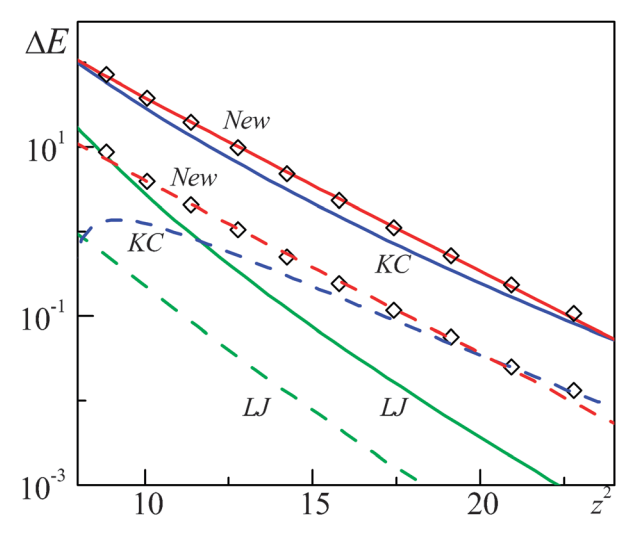


Fig. 2 Calculated relative energies ΔE_{AA} (solid lines; in meV per atom) and ΔE_{SP} (dashed lines; in meV per atom) of the AA and SP stackings of bilayer graphene as functions of the square of the interlayer spacing z^2 (in \mathring{A}^2) for different potentials: Lennard-Jones potential (LJ), Kolmogorov-Crespi potential (KC) and potential developed in the present work (New). The results of the DFT-D calculations (rhombs) are shifted by the difference of the equilibrium interlayer spacings for bilayer graphene obtained using the developed potential and DFT-D.

in agreement with the experiment. 46 The potential relief of the interlayer interaction energy of bilayer graphene is characterized by the following two quantities. The first quantity is the magnitude of corrugation of the potential relief $\Delta E_{\rm AA} = E_{\rm AA} - E_{\rm AB}$. The second one is the energy barrier for transition of the layers between adjacent energy minima represented by the AB stacking $\Delta E_{SP} = E_{SP} - E_{AB}$, where

 $E_{\rm SP}$ is the interaction energy corresponding to the saddle point stacking (SP stacking) (see Fig. 1). These two quantities are referred to below as the relative energies ΔE_{AA} and ΔE_{SP} of the AA and SP stackings, respectively.

Convergence on the number of k-points in the Brillouin zone and the maximum kinetic energy of plane waves was tested for bilayer graphene with respect to the interlayer binding energy E_{AB} and relative energies of the AA and SP stackings ΔE_{AA} and ΔE_{SP} at the equilibrium interlayer spacing (see Table 1). It is seen that accuracies of about 0.6%, 0.7% and 1.6% in calculations of the interlayer binding energy E_{AB} , the relative energies $\Delta E_{\rm AA}$ and $\Delta E_{\rm SP}$ of the AA and SP stackings, respectively, are reached for the 24 \times 36 \times 1 k-point sampling and a cutoff energy of 400 eV. In calculations for bulk graphite, a similar accuracy is achieved using the $24 \times 36 \times 16$ k-point sampling.

Let us consider the dependence of the interlayer interaction energy on the distance between the graphene layers. The calculations for bilayer graphene with the original PBE functional showed only a small energy minimum corresponding to an interlayer binding energy of -1.12 meV per atom at an interlayer spacing of 4.45 Å. As opposed to the original PBE functional, the PBE-D functional provides a binding energy of the graphene layers of -50.6 meV per atom at an interlayer spacing of 3.25 Å (see Table 2).

The PBE-D functional was found to closely reproduce the experimental data on the interlayer binding energy, 20-22 interlayer spacing 16,17 and c-axis compressibility 18 of graphite (see Table 3), in agreement with ref. 30. However, the values of the interlayer binding energy and c-axis compressibility obtained in the present paper differ by about 5% from the ones reported in ref. 30. In paper 30, the PWscf code from the Quantum-ESPRESSO package⁴⁷ with ultrasoft pseudopotentials⁴⁸ and the $12 \times 12 \times 8$ k-point sampling was used. So the small discrepancy of the results can be explained by the differences in the computational approaches (particularly, the fewer number of k-points used in calculations in ref. 30).

The relative energies ΔE_{AA} and ΔE_{SP} of the AA and SP stackings for bilayer graphene at the equilibrium interlayer spacing are given in Table 2. It should be noted that the calculated barrier for transition of the layers between adjacent energy minima exceeds the maximum values of the barriers for relative motion of carbon nanotube walls 14,36,49-52 reached for commensurate non-chiral nanotube walls by one-two orders of magnitude. This is due to perfect matching between the graphene layers as opposed to the curved nanotube walls.

The values of ΔE_{AA} and ΔE_{SP} obtained here are nearly twice higher than those reported earlier, $\Delta E_{\rm AA} \approx 10$ –15 meV per atom, $\Delta E_{\rm SP} \approx 1$ meV per atom (see ref. 32, 35, 36). Let us discuss possible reasons for this discrepancy. In papers 35, 36, the calculations of $\Delta E_{\rm AA}$ and $\Delta E_{\rm SP}$ were performed for graphite under periodic boundary conditions. The VASP code³⁷ with ultrasoft pseudopotentials⁴⁸ and the LDA functional⁵³ was used, the cutoff energy was 358 eV, and the number of k-points was not specified. We believe that those calculations^{35,36} of the potential relief of the interlayer energy did not reach the accuracy as high as in the present work (1.6% for the relative energies of AA and SP stackings) due to the insufficient number of k-points and cutoff energy in the

Table 1 Tests for convergence on the number of k-points and cutoff kinetic energy of plane waves with respect to the interlayer binding energy E_{AB} and relative energies of the AA and SP stackings ΔE_{AA} and ΔE_{SP} in calculations with the PBE-D and PBE functionals. The calculated values correspond to the interlayer spacing 3.25 Å, which is equilibrium for the PBE-D functional

k-points	12 × 18	16×24	24×36	36×54	24×36	24×36	24×36
Energy cutoff/eV	800	800	800	800	500	400	300
PBE-D							
E_{AB}/meV per atom	-51.43	-50.91	-50.59	-50.48	-50.56	-50.80	-51.43
$\Delta E_{\rm AA}/{\rm meV}$ per atom	18.15	19.18	19.52	19.40	19.52	19.55	18.97
$\Delta E_{\rm SP}/{\rm meV}$ per atom	1.692	1.945	2.073	2.039	2.065	2.095	1.556
PBE							
E_{AB}/meV per atom	+20.51	+21.03	+21.35	+21.36	+21.39	+21.14	+20.51
$\Delta E_{\rm AA}/{\rm meV}$ per atom	17.89	19.04	19.41	19.28	19.40	19.44	18.86
$\Delta E_{\rm SP}/{\rm meV}$ per atom	1.721	1.973	2.102	2.067	2.093	2.123	1.585

Table 2 Calculated interlayer binding energy E_{AB} , equilibrium interlayer spacing c_0 , compressibility χ , relative energies of the AA and SP stackings ΔE_{AA} and ΔE_{SP} , frequency of the small relative translational vibrations of the layers f_0 , parameters U_0 and U_1 for approximation (2) of the potential relief of the interlayer interaction energy and relative root-mean-square deviation of approximation (2) $\delta U/U_1$ at the equilibrium interlayer spacing for bilayer graphene

	DFT-D	vdW-DF	New potential	KC potential	LJ potential
E_{AB}/meV per atom	-50.6	-29.3	-46.90	-43.69	-45.67
$c_0/{ m \AA}$	3.25	3.35	3.374	3.375	3.384
$c_0/\text{Å} \ \chi/\text{GPa}^{-1}$	0.0257		0.0261	0.0309	0.0308
$\Delta E_{\rm AA}/{\rm meV}$ per atom	19.5	18.9	19.5	13.3	0.887
$\Delta E_{\rm SP}/{\rm meV}$ per atom	2.07	1.92	2.07	0.841	0.0809
f_0/THz	1.04		1.06	0.539	0.213
U_0 /meV per atom	-50.59		-46.90	-43.69	-45.67
U_1/meV per atom	4.24		4.24	2.14	0.178
$\delta {U}/U_1$	0.043		0.044	0.87	0.21

Table 3 Calculated interlayer binding energy E_{AB} , equilibrium interlayer spacing c_0 , compressibility χ and frequency of the small relative translational vibrations of the layers f_0 at the equilibrium interlayer spacing for graphite

	DFT-D	New potential	KC potential	LJ potential	Exp
E_{AB}/meV per atom	-57.1	-52.0	-48.8	-52.0	52^{+5a}_{-5} , 43^b , 35^{+15c}_{-10}
	3.22	3.341	3.336	3.340	3.328^d , 3.354^e
$c_0/\text{Å} \ \chi/\text{GPa}^{-1}$	0.0225	0.0244	0.0270	0.0256	0.024^{f}
f_0/THz	1.50	1.58	0.807	0.335	$\sim 1.5^g$
^a Ref. 22. ^b Ref. 21. ^c Ref. 20. ^d Ref. 16. ^e Ref. 17. ^f Ref. 18. ^g Ref. 19.					

calculations. Moreover, the discrepancy in the values of $\Delta E_{\rm AA}$ and $\Delta E_{\rm SP}$ obtained here and in works 35, 36 can be attributed to the use of the different functionals. In paper 32, the calculations of interaction of polycyclic aromatic molecules with a graphene flake were performed using the Q-Chem quantum chemistry package⁵⁴ with the $\omega B97X$ -D functional. ⁵⁵ In this case, the discrepancy in the values of $\Delta E_{\rm AA}$ and $\Delta E_{\rm SP}$ can be related to the strong influence of the edge effects³² in the finite systems, and the use of the different version of the DFT-based approach.

In order to check the validity of our results obtained using the DFT functional with the empirical dispersion correction, we also performed calculations of potential energy relief of bilayer graphene using the vdW-DF functional ³³ implemented in the GPAW code. ⁵⁶ These calculations were performed using the real space grid with spacing 0.12 Å and the same size of the model cell as in the above DFT-D calculations. Integration in the inverse space was carried out using the 18 × 27 × 1 *k*-point sampling. The results obtained with the vdW-DF functional are given in Table 2 in comparison with those for the DFT-D functional. It is seen that both functionals give approximately

the same values of the characteristics $\Delta E_{\rm AA}$ and $\Delta E_{\rm SP}$ of the potential relief of the interlayer interaction energy for bilayer graphene. Note also that the vdW-DF functional is not accurate with respect to the interlayer binding energy of bilayer graphene. So at the moment the vdW-DF approach is yet not more reliable than DFT-D.

Though the dispersion term strongly affects the overall interlayer binding energy, the contributions of the dispersion term to the barrier for relative motion of graphene layers $\Delta E_{\rm SP}$ and the magnitude of corrugation of the potential relief of the interlayer interaction energy $\Delta E_{\rm AA}$ were found to be only 1.4% and 0.6%, respectively. The characteristics of the potential relief of the interaction energy of graphene layers are mostly determined by the overlap of electron clouds of the layers, which is anisotropic and strongly dependent on the relative position of the layers as opposed to the long-range dispersion forces. So we confirmed the qualitative conclusion of paper 32 made for polycyclic aromatic molecules on a graphene flake that the dispersion correction provides a small contribution (<10%) to the magnitude of corrugation of the potential relief of the interlayer interaction energy for

graphene-like layers $\Delta E_{\rm AA}$. Evaluation of the contribution of the dispersion correction to the barrier for relative motion of graphene layers ΔE_{SP} in paper 32 was complicated due to the influence of the edge effects. According to our calculations, this contribution is also negligibly small. Therefore, such a correction is not relevant for consideration of relative motion of graphene layers.

The calculated dependences of the relative energies ΔE_{AA} and ΔE_{SP} of the AA and SP stackings on the interlayer spacing are shown in Fig. 2. These dependences can be approximated as $\Delta E_{\rm AA}$, $\Delta E_{\rm SP} \propto \exp(-\lambda_2 z^2)$ with $\lambda_2 \approx 0.464 \, {\rm A}^{-2}$, where z is the interlayer spacing.

The frequency f_0 of the small relative translational vibrations of the graphene layers about the energy minimum (see Table 2) was found as

$$f_0 = \frac{1}{2\pi} \sqrt{\frac{2}{m}} \frac{\partial^2 U}{\partial x^2},\tag{1}$$

where U is the potential energy per atom of one of the layers, $\partial^2 U/\partial x^2$ is the second derivative of the potential energy with respect to the displacement along the armchair direction at the energy minimum and m is the mass of a carbon atom. A similar quantity for graphite is given in Table 3 and is consistent with the experimental value for the frequency of TO' mode of graphite at Γ-point of about 1.5 THz (see ref. 19).

It should also be mentioned that in papers on superlubricity of graphene (see, e.g., ref. 6 and 8), the interaction of a single carbon atom in the graphene flake with the graphite surface was described using the simple approximation⁵⁷ containing only the first Fourier components. Based on that expression, it is easy to show that the potential energy relief of bilayer graphene can be roughly approximated in the form

$$U = U_1(z) \left(1.5 + \cos \left(2k_1 x - \frac{2\pi}{3} \right) -2\cos \left(k_1 x - \frac{\pi}{3} \right) \cos(k_2 y) \right) + U_0(z)$$
(2)

where $k_2 = 2\pi/a_0$, $k_1 = k_2/\sqrt{3}$, x and y axes are chosen along the armchair and zigzag directions, respectively, $U_1(z)$ and $U_0(z)$ are expressed through the parameters $V_1(z)$ and $V_0(z)$ of paper 6 as $U_1(z) = 0.5V_0(z)$ and $U_0(z) = V_1(z) - 0.75V_0(z)$. The parameters U_0 , U_1 fitted to reproduce the potential energy relief of bilayer graphene for the equilibrium interlayer spacing and relative root-mean-square deviation $\delta U/U_1$ of approximation (2) from the potential energy relief obtained using the DFT-D calculations are given in Table 2. Though approximation (2) is rather simple, it can be fitted to reproduce the potential energy relief of bilayer graphene obtained through the DFT-D calculations with the accuracy of a few percent. Therefore, such approximations are adequate for interpretation^{6,8} of the experiments on superlubricity of graphene using the friction force microscope. The value of the parameter $U_1 = 0.5V_0 \approx 4.24$ meV per atom fitted to reproduce the results of our DFT-D calculations is in reasonable agreement with the values of the parameter $V_0 \approx 3.3-6.7$ meV per atom fitted to the experimental data obtained using the friction force microscope.^{6,8}

Classical potential for interaction between graphene layers

It was pointed out in papers 35, 36 that the π -overlap between graphene layers is anisotropic. So to fit both the experimental graphite compressibility and the corrugation against sliding, it is needed to distinguish the in-plane and out-of-plane directions. This approach was firstly realized in the Kolmogorov-Crespi potential.^{35,36} We used such an approach to develop a new classical potential for the interaction of graphene layers on the basis of the results of our DFT-D calculations.

We assumed that the interaction of atoms of the layers at a distance r, transverse separation ρ and interlayer spacing z $(r^2 = \rho^2 + z^2)$ can be described as

$$U = A \left(\frac{z_0}{r}\right)^6 + B \exp(-\alpha(r - z_0))$$

+ $C(1 + D_1 \rho^2 + D_2 \rho^4) \exp(-\lambda_1 \rho^2) \exp(-\lambda_2 (z^2 - z_0^2))$
(3)

where $z_0 = 3.34 \text{ Å}$ is the equilibrium interlayer spacing of graphite.

The potential consists of two parts. The first part is isotropic. The parameters of this part A = -10.510 meV, B = 11.652 meV and $\alpha = 4.16 \text{ Å}^{-1}$ were fitted to provide the interlayer binding energy,²² interlayer spacing^{16,17} and *c*-axis compressibility¹⁸ for graphite close to the recent experimental values (see Table 3). As this part of the potential was fitted to the experimental data, it provides the equilibrium interlayer spacing of bilayer graphene $d_{\rm eq}=3.38$ Å, which is greater than the equilibium interlayer spacing following from the DFT-D calculations $d_{eq} = 3.25 \text{ Å}$ (see Table 2). The second part of the potential is anisotropic and determines the dependence of the interlayer energy on the in-plane relative displacement of graphene layers. The parameters of the second part of the potential were fitted to satisfy the following conditions: (1) this part gives zero contribution to the interlayer interaction energy for the AB stacking; (2) the relative energies ΔE_{AA} and ΔE_{SP} of the AA and SP stackings and the frequency of the small relative translational vibrations of the layers f_0 at the equilibrium interlayer spacing d_{eq} = 3.38 Å have the same values as were provided by the DFT-D calculations for $d_{\rm eq} = 3.25$ Å. The following values of the parameters were obtained: C = 35.883 meV, $D_1 =$ -0.86232 Å^{-2} , $D_2 = 0.10049 \text{ Å}^{-4}$ and $\lambda_1 = 0.48703 \text{ Å}^{-2}$ (see Fig. 1). To provide the dependences of the relative energies ΔE_{AA} and ΔE_{SP} of the AA and SP stackings on the interlayer spacing following from the DFT-D calculations the parameter λ_2 was set equal to $\lambda_2 = 0.46445 \text{ Å}^{-2}$ (see Fig. 2). For the fitting procedure and the MD simulations presented below, the cutoff distance of the potential was taken equal to 25 A. It is seen that the fitting procedure is rather simple and can be easily applied to revise the parameters of the potential as soon as the experimental data on the potential relief of the interlayer interaction energy in graphite or few-layer graphene become available.

The root-mean square deviation of the potential energy relief for the fitted potential (3) from the potential energy relief obtained using the DFT-D calculations is 0.17 meV per atom, which is only 0.8% of the magnitude of corrugation of the potential relief of the interlayer interaction energy $\Delta E_{\rm AA}$. The frequency of the small relative vibrations of the graphene layers exceeds the DFT-D value only by 2% (see Table 2).

The first version of the Kolmogorov–Crespi potential³⁵ gives the energy minimum for bilayer graphene at the SP-stacking. The second version of the Kolmogorov–Crespi potential³⁶ provides the qualitatively correct behavior of the interlayer interaction energy. However, it displays a significant root-mean-square deviation from the potential energy relief obtained using our DFT-D calculations of about 2.6 meV per atom (see Fig. 1).

The form of the potential (3) is similar to that of the Kolmogorov–Crespi potential. 35,36 However, we modified the dependence of the anisotropic part of the potential on the interlayer spacing z to reproduce the dependences of the relative energies $\Delta E_{\rm AA}$ and $\Delta E_{\rm SP}$ of the AA and SP stackings on the interlayer spacing obtained using the DFT-D calculations (see Fig. 2). According to our DFT-D results, these dependences are approximated by $\exp(-\lambda_2 z^2)$ better than by $\exp(-\lambda_3 z)$. The Kolmogorov–Crespi potential 36 gives the dependence of the barrier to relative motion of graphene layers $\Delta E_{\rm SP}$ on the interlayer spacing essentially different from the dependence found from our DFT-D calculations (see Fig. 2).

Furthermore, we found that to fit the relative energies ΔE_{AA} and ΔE_{SP} of the AA and SP stackings and the frequency of the small relative translational vibrations of the layers f_0 obtained using the developed potential to the values following from our DFT-D calculations at the same time it was necessary to increase the contribution of long-distance atoms of the opposite layer. In consequence of this, we obtained a relatively low value of the parameter λ_1 for the developed potential, so that long-distance atoms separated from a considered atom by the distance up to three bond lengths of graphene in the transverse direction contribute to the anisotropic part of the potential. This is opposed to the Kolmogorov-Crespi potential^{35,36} for which the main contribution to the anisotropic part is provided by the nearest atoms of the opposite layer within the distance corresponding to a single bond length in the transverse direction.

The Lennard-Jones potential

$$U_{\rm LJ} = 4\varepsilon \left(\left(\frac{\sigma}{r} \right)^{12} - \left(\frac{\sigma}{r} \right)^{6} \right) \tag{4}$$

was also considered for comparison. The parameters of the Lennard-Jones potential $\varepsilon=2.757$ meV, $\sigma=3.393$ Å were fitted to reproduce the interlayer binding energy, interlayer spacing 16,17 and c-axis compressibility 18 for graphite. The cutoff distance of the potential was equal to 25 Å. Though the Lennard-Jones potential reproduces the experimental data 16-18,22 for graphite, the magnitude of corrugation of the potential relief of the interlayer interaction energy is underestimated by an order of magnitude (see Fig. 1, Fig. 2 and Table 2).

As the in-plane and out-of-plane directions should be distinguished in order to fit both the experimental graphite compressibility and the corrugation against sliding, any pairwise potential similar to the Lennard-Jones potential also strongly underestimates the magnitude of corrugation of the

potential relief of the interlayer interaction energy in graphite or few-layer graphene. In particular, we performed the calculations of the potential energy relief for bilayer graphene using the MM3 and MM4 force fields. ^{58,59} The calculations showed that for these potentials, the minimum of the interlayer binding energy of -49.54 meV per atom is reached at an interlayer spacing of 3.433 Å. At this interlayer spacing, the magnitude of corrugation of the potential energy relief of bilayer graphene and the barrier for relative motion of the layers are only $\Delta E_{\rm AA} = 0.510$ meV per atom and $\Delta E_{\rm SP} = 0.0542$ meV per atom, respectively. These values are more than an order of magnitude smaller than the results of the DFT-D calculations, similar to the Lennard-Jones potential (see Fig. 1, Fig. 2 and Table 2).

4. MD simulations of the graphene-based nanoresonator

To investigate the influence of the potential on dynamic behavior of graphene-based systems, we performed simulations of the nanoresonator based on the small relative translational vibrations of graphene layers similar to the recently proposed ultra-high frequency nanoresonator based on the small relative vibrations of carbon nanotube walls. 14,15 We compared the dynamic behavior of the systems in which the interlayer interaction is described using three different potentials: the potential developed in the present work, Kolmorogov-Crespi³⁶ and Lennard-Jones potentials. The system used in the MD simulations consisted of two infinite graphene layers. The size of the model cell was $5.1 \text{ nm} \times 5.2 \text{ nm}$. The periodic boundary conditions were applied along mutually perpendicular armchair and zigzag directions of the graphene layers. The covalent carbon-carbon interactions in the layers were described by the empirical Brenner potential,60 which was shown to correctly reproduce the vibrational spectra of carbon nanotubes⁶¹ and graphene nanoribbons⁶² and has been widely applied to study carbon systems. 10,14,63-65 Microcanonical MD simulations of the small vibrations of the graphene layers were performed at the liquid helium temperature 4.2 K and at the liquid nitrogen temperature 77 K. An in-house MD-kMC code⁶⁶ was implemented. The code used the velocity Verlet algorithm. The integration time step was 0.4 fs. The simulation time was 0.5-1.0 ns. To start the vibration, one of the layers was shifted by 0.2 Å from the energy minimum in the armchair direction and released with zero center-of-mass velocity. During the simulations, both of the layers were free.

The relative displacement of the centers of mass of the layers as a function of time is shown in Fig. 3. To estimate the frequency and the Q-factor of the vibrations, the Fourier transform of the relative displacement of the centers of mass of the layers was calculated (see Fig. 4). The frequency f of the vibrations was found as the center of the main peak and the Q-factor was estimated by the width Δf of the peak as

$$Q = \frac{f}{2\pi\Delta f}. (5)$$

The frequencies of the vibrations and the Q-factors obtained through the MD simulations using different potentials are

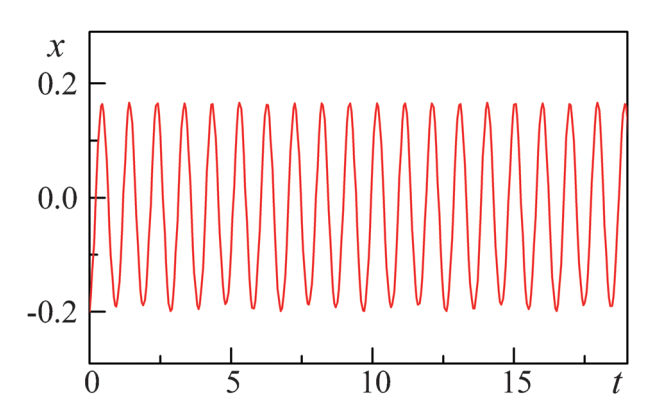


Fig. 3 Relative position x (in Å) of the centers of mass of the graphene layers as a function of time t (in ps) at temperature 4.2 K calculated using the potential developed in the present work.

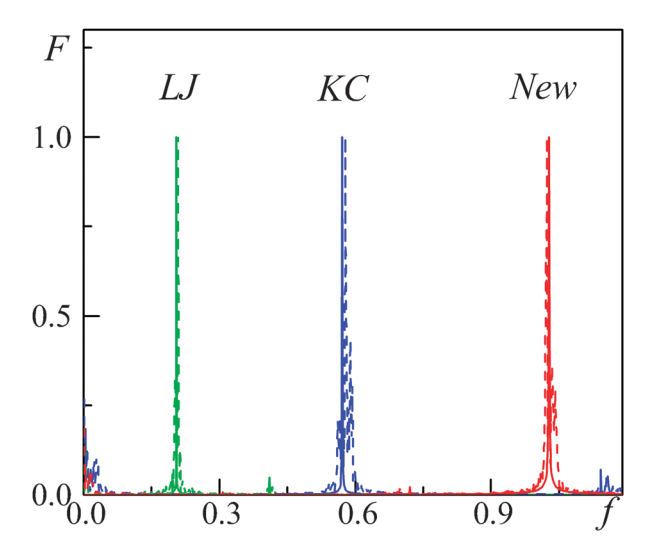


Fig. 4 Calculated Fourier transforms of the relative displacement of the graphene layers along the armchair direction at temperatures 4.2 K (solid lines) and 77 K (dashed lines) for different potentials: Lennard-Jones potential (LJ), Kolmogorov–Crespi potential (KC) and potential developed in the present work (New). Frequency f is given in THz.

Table 4 Calculated frequency f and Q-factor Q of the nanoresonator based on the small relative translational vibrations of graphene layers at temperatures 4.2 K and 77 K

Potential	New potential	KC potential	LJ potential
T = 4.2 K f/THz Q $T = 77 K$	$\begin{array}{c} 1.0278 \pm 0.0005 \\ 150 \pm 80 \end{array}$	$0.5811 \pm 0.0004 \\ 110 \pm 80$	$0.2051 \pm 0.0004 \\ 40 \pm 30$
f/THz Q	$\begin{array}{c} 1.0236 \pm 0.0012 \\ 70 \pm 30 \end{array}$	$\begin{array}{c} 0.5774 \pm 0.0011 \\ 41 \pm 16 \end{array}$	$\begin{array}{c} 0.2087 \pm 0.0008 \\ 21 \pm 12 \end{array}$

listed in Table 4. The frequencies of the relative translational vibrations of the graphene layers observed in the MD simulations (see Table 4) are in agreement with the values derived from the steepness of the minima of the calculated potential relief of the interlayer interaction energy (see Table 2). The small discrepancy is related to anharmonicity of the vibrations of the considered amplitude. As it is seen from Table 4, the

O-factor of the graphene-based nanoresonator is relatively small, $Q \approx 10$ –100, for all the considered potentials. The Q-factor strongly decreases with temperature.

The small O-factor values of the nanoresonator are related to the intensive energy exchange of the considered relative vibrations of the graphene layers with other vibrational modes. The relative translational vibrations of the layers are excited in the direction perpendicular to the considered vibrations (but parallel to the layer). This is due to degeneracy of the vibrations in the perpendicular directions, which is a result of the graphene symmetry. The excitation of the vibrations in the perpendicular direction is an intrinsic property of graphene and is not sensitive to the choice of the potential.

Furthermore, the high dissipation in the nanoresonator can be provided also by the excitation of other low frequency vibrational modes, such as the flexural vibrations of the graphene layers. The fundamental frequency of the flexural vibrations of the layers can be found as

$$f_{\rm b} = \frac{2\pi c_{\rm b}}{L^2},\tag{6}$$

where the coefficient c_b was found to be $c_b = 5.6 \times 10^{-7} \,\mathrm{m}^2 \,\mathrm{s}^{-1}$ (see ref. 67) and L is the length of the graphene layers (or the length of the model cell in our simulations). The effective excitation of the flexural vibrations should be observed at $f_{\rm b} \leq f$, i.e. for lengths L > 2 nm for the developed potential and L > 3 nm for the Kolmogorov–Crespi potential.

It is seen from Table 4 and Fig. 4 that the dynamic behavior of the nanoresonator is strongly influenced by the choice of the potential. The developed potential provides the highest frequency of the small relative translational vibrations of the graphene layers, as it follows from the performed DFT-D calculations. Furthermore, the Q-factor is in general higher for the developed potential compared to those for the Kolmogorov-Crepsi and Lennard-Jones potentials (see Table 4).

The degeneracy of the translational vibrations in the perpendicular directions and fast energy transfer to the flexural vibrations of the graphene layers provide the relatively small Q-factor values for the nanoresonator based on the relative translational vibrations of the graphene layers. This is opposed to the nanoresonator based on the relative vibrations of the walls of the (9,0)@(18,0) carbon nanotube, for which the high Q-factor values ($Q \approx 500$ at the liquid helium temperature 4.2 K and $Q \approx 200$ at the liquid nitrogen temperature 77 K) were obtained using the Lennard-Jones potential. Carbon nanotubes are one-dimensional structures, so the translational vibrations of the walls along the axis are not degenerate. Since nanotubes are stiffer than graphene, the flexural vibrations of nanotubes should get in the resonance with the translational vibrations of the walls and, therefore, become important for energy dissipation only at long nanotube lengths (the analogous conclusion was drawn for nanotube-based gigahertz oscillators). 64 This explains high Q-factor values for the nanoresontators based on the relative vibrations of nanotube walls as compared to the nanoresontators based on the relative vibrations of graphene layers.

The low Q-factor values for the nanoresonator based on the small relative translational vibrations of graphene layers demonstrate that graphene is not suitable for such an application. However, this allows elaborating the nanorelays and memory cells which are based on relative motion of graphene layers and are fast-responding due to fast damping of mechanical oscillations after switching.

5. Conclusions

The potential relief of the interlayer interaction energy of bilayer graphene was investigated in the framework of the DFT-D approach using the recent PBE-D functional. Based on the methodological study, it was found that the $24 \times 36 \times 1$ k-point sampling and a cutoff energy of 400 eV are required to achieve the sufficient accuracy of calculations. This allowed us to revise the results of the previous DFT calculations without the dispersion correction. 35,36 In particular, the magnitude of corrugation of the potential relief of the interlayer interaction energy for bilayer graphene ΔE_{AA} and the barrier for relative motion of graphene layers ΔE_{SP} were found to be ΔE_{AA} = 19.5 meV per atom and $\Delta E_{\rm SP} = 2.07$ meV per atom. The contributions of the dispersion correction to quantities $\Delta E_{\rm SP}$ and $\Delta E_{\rm AA}$ were shown to be 1.4% and 0.6%, respectively. So though the dispersion term strongly affects the overall interlayer binding energy, the influence of the dispersion term on relative motion of graphene layers is negligible. This conclusion is also of high importance for carbon nanotubes, for which a number of DFT calculations of the barriers to relative motion of nanotube walls were performed without the dispersion correction. 14,36,49-52

It was also shown that the results of the DFT-D calculations can be fitted with sufficient accuracy using the simple expression for interaction of graphene layers containing only the first Fourier components (see eqn (2)). Therefore, such approximations are adequate for interpretation^{6,8} of the experiments on superlubricity of graphene using the friction force microscope.

Based on the DFT-D calculations, a new classical potential for the interaction between graphene layers was developed. The potential accurately reproduces the experimental data on the interlayer binding energy, interlayer spacing, *c*-axis compressibility of graphite as well as the data obtained from the DFT-D calculations on the magnitude of corrugation of the interlayer interaction energy, barrier for relative motion of graphene layers and frequency of the small relative translational vibrations of graphene layers. Therefore, the developed potential should be useful for modeling graphene-based nanodevices, ^{2,11} superlubricity ⁶⁻⁹ and diffusion ¹⁰ of graphene flakes, ripples, ⁵ thermal conductivity ⁴ and mechanical properties of few-layer graphene. ³

The influence of the choice of the classical potential on the dynamic properties of graphene-based systems was investigated by the example of the nanoresonator based on the small relative translational vibrations of graphene layers. The MD simulations of the graphene-based nanoresonator were performed using the potential developed in the present work, Kolmogorov–Crespi^{35,36} and Lennard-Jones potentials for the interlayer interaction. The developed potential was found to provide the highest frequency of the relative translational vibrations of the graphene layers and the highest value of the *Q*-factor. The calculated low values of the *Q*-factor of the

graphene-based nanoresonator $Q \approx 10$ –100 show that graphene should be perfect for the use in fast-responding nanorelays and nanoelectromechanical memory cells, for which fast dissipation of mechanical oscillations after switching is necessary.

Acknowledgements

This work has been partially supported by the RFBR grants 11-02-00604 and 10-02-90021-Bel.

Notes and references

- K. S. Novoselov, A. K. Geim, S. V. Morozov, D. Jiang, Y. Zhang, S. V. Dubonos, I. V. Grigorieva and A. A. Firsov, *Science*, 2004, 306, 666.
- 2 S. Bae, H. Kim, Y. Lee, X. Xu, J.-S. Park, Y. Zheng, J. Balakrishnan, T. Lei, H. R. Kim, Y. I. Song, Y.-J. Kim, K. S. Kim, B. Ozyilmaz, J.-H. Ahn, B. H. Hong and S. Iijima, Nat. Nanotechnol., 2010, 5, 574.
- 3 D. A. Dikin, S. Stankovich, E. J. Zimney, R. D. Piner, G. H. B. Dommett, G. Evmenenko, S. B. T. Nguyen and R. S. Ruoff, *Nature*, 2007, **448**, 457.
- 4 S. Ghosh, W. Bao, D. L. Nika, S. Subrina, E. P. Pokatilov, Ch. N. Lau and A. A. Balandin, *Nat. Mater.*, 2010, **9**, 555.
- 5 J. C. Meyer, A. K. Geim, M. I. Katsnelson, K. S. Novoselov, D. Obergfell, S. Roth, C. Girit and A. Zettl, *Solid State Commun.*, 2007, 143, 101.
- 6 G. S. Verhoeven, M. Dienwiebel and J. W. M. Frenken, *Phys. Rev. B: Condens. Matter*, 2004, 70, 165418.
- 7 M. Dienwiebel, G. S. Verhoeven, N. Pradeep, J. W. M. Frenken, J. A. Heimberg and H. W. Zandbergen, *Phys. Rev. Lett.*, 2004, 92, 126101.
- 8 A. E. Filippov, M. Dienwiebel, J. W. M. Frenken, J. Klafter and M. Urbakh, *Phys. Rev. Lett.*, 2008, **100**, 046102.
- N. Sasaki, K. Kobayashi and M. Tsukada, Phys. Rev. B: Condens. Matter, 1996, 54, 2138.
- 10 I. V. Lebedeva, A. A. Knizhnik, A. M. Popov, O. V. Ershova, Yu. E. Lozovik and B. V. Potapkin, *Phys. Rev. B: Condens. Matter*, 2010, 82, 155460.
- 11 Q. Zheng, B. Jiang, S. Liu, Yu. Weng, L. Lu, Q. Xue, J. Zhu, Q. Jiang, S. Wang and L. Peng, *Phys. Rev. Lett.*, 2008, **100**, 067205.
- 12 V. V. Deshpande, H.-Y. Chiu, H. W. Ch. Postma, C. Miko, L. Forro and M. Bockrath, *Nano Lett.*, 2006, 6, 1092.
- 13 A. Subramanian, L. X. Dong, B. J. Nelson and A. Ferreira, *Appl. Phys. Lett.*, 2010. **96**, 073116.
- 14 E. Bichoutskaia, A. M. Popov, Yu. E. Lozovik, O. V. Ershova, I. V. Lebedeva and A. A. Knizhnik, *Phys. Rev. B: Condens. Matter*, 2009, **80**, 165427.
- E. Bichoutskaia, A. M. Popov, Yu. E. Lozovik, O. V. Ershova,
 I. V. Lebedeva and A. A. Knizhnik, Fullerenes, Nanotubes, and Carbon Nanostruct., 2010, 18, 523.
- 16 A. Ludsteck, Acta. Crystallogr., Sect. A: Cryst. Phys., Diffr., Theor. Gen. Crystallogr., 1972, 28, 59.
- 17 Y. X. Zhao and I. L. Spain, Phys. Rev. B: Condens. Matter, 1989, 40, 993.
- 18 W. B. Gauster and I. J. Fritz, J. Appl. Phys., 1974, 45, 3309.
- 19 R. Nicklow, N. Wakabayashi and H. G. Smith, Phys. Rev. B: Condens. Matter, 1972, 5, 4951.
- 20 L. X. Benedict, N. G. Chopra, M. L. Cohen, A. Zettl, S. G. Louie and V. H. Crespi, *Chem. Phys. Lett.*, 1998, **286**, 490.
- 21 L. A. Girifalco and R. A. Lad, J. Chem. Phys., 1956, 25, 693.
- 22 R. Zacharia, H. Ulbricht and T. Hertel, *Phys. Rev. B: Condens. Matter*, 2004, **69**, 155406.
- 23 D. E. Soule and C. W. Nezbeda, J. Appl. Phys., 1968, 39, 5122.
- 24 L. A. Girifalco and M. Hodak, Phys. Rev. B: Condens. Matter, 2002, 65, 125404.
- 25 H. Rydberg, M. Dion, N. Jacobson, E. Schroder, P. Hyldgaard, S. I. Simak, D. C. Langreth and B. I. Lundqvist, *Phys. Rev. Lett.*, 2003. 91, 126402.
- 26 M. Hasegawa and K. Nishidate, *Phys. Rev. B: Condens. Matter*, 2004, **70**, 205431.

- 27 X. Wu, M. C. Vargas, S. Nayak, V. Lotrich and G. Scoles, J. Chem. Phys., 2001, 115, 8748.
- 28 M. Hasegawa, K. Nishidate and H. Iyetomi, Phys. Rev. B: Condens. Matter, 2007, 76, 115424.
- F. Ortmann, F. Bechstedt and W. G. Schmidt, Phys. Rev. B: Condens. Matter, 2006, 73, 205101.
- V. Barone, M. Casarin, D. Forrer, M. Pavone, M. Sambi and A. Vittadini, J. Comput. Chem., 2008, 30, 934.
- 31 S. Grimme, J. Comput. Chem., 2006, 27, 1787.
- 32 O. V. Ershova, T. C. Lillestolen and E. Bichoutskaia, Phys. Chem. Chem. Phys., 2010, 12, 6483.
- M. Dion, H. Rydberg, E. Schröder, D. C. Langreth and B. I. Lundqvist, Phys. Rev. Lett., 2004, 92, 246401.
- 34 X. Wu, M. C. Vargas, S. Nayak, V. Lotrich and G. Scoles, J. Chem. Phys., 2001, 115, 8748.
- 35 A. N. Kolmogorov and V. H. Crespi, Phys. Rev. Lett., 2000, 85, 4727.
- 36 A. N. Kolmogorov and V. H. Crespi, Phys. Rev. B: Condens. Matter, 2005, 71, 235415.
- 37 G. Kresse and J. Furthmüller, Phys. Rev. B: Condens. Matter, 1996, 54, 11169.
- 38 J. P. Perdew, K. Burke and M. Ernzerhof, Phys. Rev. Lett., 1996, 77, 3865.
- 39 G. Kresse and D. Joubert, Phys. Rev. B: Condens. Matter, 1999, **59**, 1758.
- 40 H. J. Monkhorst and J. D. Pack, Phys. Rev. B: Solid State, 1976,
- 41 E. R. Davidson, in Methods in Computational Molecular Physics, Vol. 113 of NATO Advanced Study Institute, Series C, ed. G. H. F. Diercksen and S. Wilson, Plenum, New York, 1983, p. 95.
- 42 M. Methfessel and A. T. Paxton, Phys. Rev. B: Condens. Matter, 1989, 40, 3616.
- 43 A. V. Belikov, Yu. E. Lozovik, A. G. Nikolaev and A. M. Popov, Chem. Phys. Lett., 2004, 385, 72.
- 44 Yu. E. Lozovik and A. M. Popov, Chem. Phys. Lett., 2000, 328,
- 45 Yu. E. Lozovik and A. M. Popov, Phys. Solid State, 2002, 44, 186.
- 46 Y. Gamo, A. Nagashima, M. Wakabayashi, M. Terai and C. Oshima, Surf. Sci., 1997, 374, 61.
- 47 http://www.pwscf.org/
- 48 D. Vanderbilt, Phys. Rev. B: Condens. Matter, 1990, 41, 7892.

- 49 A. M. Popov, Yu. E. Lozovik, A. S. Sobennikov and A. A. Knizhnik, J. Exp. Theor. Phys., 2009, 108, 621
- 50 J.-C. Charlier and J. P. Michenaud, Phys. Rev. Lett., 1993, 70, 1858.
- 51 E. Bichoutskaia, M. I. Heggie, A. M. Popov and Y. E. Lozovik, Phys. Rev. B: Condens. Matter, 2006, 73, 045435.
- 52 E. Bichoutskaia, A. M. Popov, A. El-Barbary, M. I. Heggie and Y. E. Lozovik, Phys. Rev. B: Condens. Matter, 2005, 71, 113403.
- 53 J. P. Perdew and A. Zunger, Phys. Rev. B: Condens. Matter, 1981, **23**, 5048.
- 54 J. Kong, C. A. White, A. I. Krylov, C. D. Sherrill, R. D. Adamson, T. R. Furlani, M. S. Lee, A. M. Lee, S. R. Gwaltney, T. R. Adams, C. Ochsenfeld, A. T. B. Gilbert, G. S. Kedziora, V. A. Rassolov, D. R. Maurice, N. Nair, Y. Shao, N. A. Besley, P. E. Maslen, J. P. Dombroski, H. Daschel, W. Zhang, P. P. Korambath, J. Baker, E. F. C. Byrd, T. Van Voorhis, M. Oumi, S. Hirata, C.-P. Hsu, N. Ishikawa, J. Florian, A. Warshel, B. G. Johnson, P. M. W. Gill, M. Head-Gordon and J. A. Pople, J. Comput. Chem., 2000, 21, 1532.
- 55 J.-D. Chai and M. Head-Gordon, Phys. Chem. Chem. Phys., 2008, 10, 6615
- 56 https://wiki.fysik.dtu.dk/gpaw/index.html.
- 57 J. W. J. Kerssemakers, Ph.D. thesis, University of Groningen, The Netherlands, 1997.
- 58 J.-H. Lii and N. L. Allinger, J. Am. Chem. Soc., 1989, 111, 8576.
- 59 N. Nevins, J.-H. Lii and N. L. Allinger, J. Comput. Chem., 1996, 17. 695.
- D. W. Brenner, O. A. Shenderova, J. A. Harrison, S. J. Stuart, B. Ni and S. B. Sinnott, J. Phys.: Condens. Matter, 2002, 14, 783.
- 61 M. Vandescuren, H. Amara, R. Langlet and Ph. Lambin, Carbon, 2007, 45, 349.
- M. Vandescuren, P. Hermet, V. Meunier, L. Henrard and Ph. Lambin, Phys. Rev. B: Condens. Matter, 2008, 78, 195401.
- 63 I. V. Lebedeva, A. A. Knizhnik, A. A. Bagatur'yants and B. V. Potapkin, *Physica E*, 2008, **40**, 589.
- 64 O. V. Ershova, I. V. Lebedeva, Yu. E. Lozovik, A. M. Popov, A. A. Knizhnik, B. V. Potapkin, O. N. Bubel, E. F. Kislyakov and N. A. Poklonskii, *Phys. Rev. B: Condens. Matter*, 2010, **81**, 155453.
- I. V. Lebedeva, A. A. Knizhnik, A. M. Popov, Yu. E. Lozovik and B. V. Potapkin, Nanotechnology, 2009, 20, 105202.
- 66 http://www.kintechlab.com/products/md-kmc/.
- 67 E. Munoz, J. Lu and B. I. Yakobson, Nano Lett., 2010, 10, 1652.